IFIC/99-73
FTUV/99-76
January 5, 2014

Bottomonium Production at the Tevatron and the LHC *

J.L. Domenech[a†] **and M.A. Sanchis-Lozano**[b,c‡]

(a) Departamento de Física Atómica, Molecular y Nuclear
(b) Instituto de Física Corpuscular (IFIC), Centro Mixto Universidad de Valencia-CSIC
(c) Departamento de Física Teórica
Dr. Moliner 50, E-46100 Burjassot, Valencia (Spain)

January 5, 2014

Abstract

Inclusive bottomonium hadroproduction at the Tevatron is firstly examined in a Monte Carlo framework with the colour-octet mechanism implemented in the event generation. We extract some NRQCD colour-octet matrix elements relevant for $\Upsilon(1S)$ hadroproduction. Remarkably we find a quite small contribution (compatible with zero) from feeddown of χ_{bJ} states produced through the colour-octet mechanism: $\Upsilon(1S)$ indirect production via χ_{bJ} decays should be mainly ascribed to the colour-singlet model. Finally we extrapolate to LHC energies to predict prompt $\Upsilon(1S)$ production rates.

PACS numbers: 12.38.Aw; 13.85.Ni
keywords: Quarkonia production; Bottomonium; Colour-Octet Model; NRQCD; Tevatron; LHC

*Research partially supported by CICYT under grant AEN99-0692
†domenech@evalo1.ific.uv.es
‡Corresponding author: mas@evalo1.ific.uv.es

1 Introduction

B-physics has been reserved an important role in the exciting programme to be developed at the Large Hadron Collider or LHC along the 21st century. As an example, the ATLAS TDR [1] collects a large number of topics related to charm and beauty flavours allowing precise tests of the Standard Model benefitting from a foreseen huge statistics even with the machine running at "low" luminosity ($\simeq 10^{33}$ cm^{-2} s^{-1}).

In a series of previous papers [2, 3, 4, 5] we examined charmonium hadroproduction in a Monte Carlo framework, using PYTHIA 5.7 [6] event generator with the colour-octet model (COM) [7] implemented in. Basically, such a production mechanism is based on the formation of an intermediate coloured state during the hard partonic interaction, evolving non-perturbatively into physical heavy resonances in the final state with certain probabilities governed by NRQCD [8]. This mechanism constitutes a (relativistic) generalization of the so-called colour-singlet model (CSM) [9] which requires the formation of a colour-singlet state in the hard interaction itself. Although the discrepancies between the CSM and experimental cross sections on bottomonia hadroproduction are smaller than those found for charmonia [10], still some extra contribution should be invoked to account for the surplus observed at the Fermilab Tevatron.

In this paper we extend our analysis on J/ψ and ψ' hadroproduction [4] to the bottomonium family lowest vector resonance, i.e. the $\Upsilon(1S)$ state. Once again, those matrix elements (MEs) determined from Tevatron data in other analysis [11] have to be lowered once initial-state radiation of gluons is taken into account. This is because of the raise of the (*effective*) intrinsic momentum (k_T) of the interacting partons enhancing the high-p_T tail of the differential cross section for heavy quarkonia production (for more details the reader is referred to Ref. [4]).

The study of bottomonia production at hadron colliders should permit a stringent test of the colour-octet production mechanism, especially regarding the expected (mainly transverse) polarization of the resonance created through this process at high-p_T. Moreover, LHC experiments will cover a wider range of transverse momentum than at the Tevatron. Therefore, it is worth to estimate, as a first step, the foreseen production rate of bottomonium resonances at the LHC and this constitutes one of the goals of this work. Thereby any experimental strategy to be conducted in the future (for example a specific high-level trigger within the dedicated B-physics data-taking) can be foreseen in advance.

We have based our study on recent results from Run 1b at the Tevatron [12]. This means significantly more statistics than the data sample from Run 1a, employed in a former analysis [11]. However, the different sources of prompt $\Upsilon(1S)$ production were not yet separated along the full accessible p_T-range, in contrast to charmonium production. Hence we give in this work numerical values for some relevant combinations of long-distance MEs (including *direct* and *indirect* $\Upsilon(1S)$ production [1]) extracted from the fit to the CDF experimental points. Nevertheless, we still are able to estimate some colour-octet MEs for *direct* production from the measurements on different production sources at $p_T > 8$ GeV [13].

[1] Prompt resonance production includes both direct and indirect channels, the latter exclusively referred to feeddown from $\Upsilon(nS)$ and $\chi_{bJ}(nP)$ states - i.e. excluding long-lived particle decays

2 Implementation of the COM in PYTHIA

Originally the event generator PYTHIA 5.7 produces direct J/ψ and higher χ_{cJ} resonances via the CSM only [6]. It is not difficult to extend this generation to the bottomonium family by redefining the resonance mass and wave function parameter accordingly. In our analysis we have besides implemented a code in the event generator to account for the colour-octet production mechanism via the following α_s^3 partonic processes [2] for heavy quarkonium production:

$$g \ + \ g \rightarrow (Q\overline{Q})[^{2S+1}X_J] \ + \ g \tag{1}$$

$$g \ + \ q \rightarrow (Q\overline{Q})[^{2S+1}X_J] \ + \ q \tag{2}$$

$$q \ + \ \overline{q} \rightarrow (Q\overline{Q})[^{2S+1}X_J] \ + \ g \tag{3}$$

where $(Q\overline{Q})[^{2S+1}X_J]$ stands for a certain heavy quarkonium state denoted by its spectroscopic notation. In particular we have considered the $^3S_1^{(8)}$, $^1S_0^{(8)}$ and $^3P_J^{(8)}$ contributions as leading-order intermediate coloured states. In addition we generated $\Upsilon(1S)$ and $\chi_{bJ}(nP)$ $(n = 1, 2)$ resonances decaying into $\Upsilon(1S)$ according to the CSM as mentioned above.

A lower p_T cut-off was set equal to 1 GeV (by default in PYTHIA) throughout the generation since some of the contributing channels are singular at vanishing transverse momentum [14].

2.1 Set of "fixed" and free parameters used in the generation

Below we list the main parameters, including masses and branching fractions, used in our generation with PYTHIA 5.7. We employed the CTEQ2L parton distribution function (PDF) in all our analysis.

Masses and branching fractions:

- $m_b = 4.88$ GeV
- $m_{resonance} = 2m_b$
- $BR[\Upsilon(1S) \rightarrow \mu^+\mu^-] = 2.48$ % ([15])

Colour-singlet parameters (from [16]):

- $< O_1^{\Upsilon(1S)}(^3S_1) > |_{tot} = 11.1$ GeV^3, defined as

$$< O_1^{\Upsilon(1S)}(^3S_1) > |_{tot} \ = \ \sum_{n=1}^{3} < O_1^{\Upsilon(nS)}(^3S_1) > Br[\Upsilon(nS) \rightarrow \Upsilon(1S)X]$$

- $< O_1^{\chi_{b1(1P)}}(^3P_1) >= 6.09$ GeV^5

[2] We find from our simulation that gluon-gluon scattering actually stands for the dominant process as expected, gluon-quark scattering contributes appreciably however ($\simeq$ 28% of the colour-octet production cross section), whereas quark-antiquark scattering represents $\simeq$ 4%. These fractions are slightly larger than those found in charmonium production as could be expected from a heavier quark mass

- $< O_1^{\chi_{b1(2P)}}(^3P_1) >= 7.10$ GeV^5

The radial wave functions at the origin (and their derivatives) used in the generation can be related to the above matrix elements as

$$< O_1^{\Upsilon(1S)}(^3S_1) > = \frac{9}{2\pi}|R(0)|^2 \tag{4}$$

$$< O_1^{\chi_{bJ(nP)}}(^3P_J) > = \frac{9}{2\pi}(2J+1)|R'(0)|^2 \tag{5}$$

whose numerical values were obtained from a Buchmüller-Tye potential model tabulated in Ref. [17].

Colour-octet long-distance parameters to be extracted from the fit:

- $< O_8^{\Upsilon(1S)}(^3S_1) > |_{tot}$, defined as

$$\begin{aligned} < O_8^{\Upsilon(1S)}(^3S_1) > |_{tot} \quad &= \sum_{n=1}^{3}\Big\{< O_8^{\Upsilon(nS)}(^3S_1) > Br[\Upsilon(nS)\to\Upsilon(1S)X] \\ &+ \sum_{J=0}^{2} < O_8^{\chi_{bJ}(nP)}(^3S_1) > Br[\chi_{bJ}(nP)\to\Upsilon(1S)X]\Big\} \end{aligned} \tag{6}$$

- $< O_8^{\Upsilon(1S)}(^1S_0) >$
- $< O_8^{\Upsilon(1S)}(^3P_0) >$

On the other hand, the differences in shape between the $^1S_0^{(8)}$ and $^3P_J^{(8)}$ contributions were not sufficiently great to justify independent generations for them. In fact, temporarily setting $< O_8^{\Upsilon(1S)}(^3P_0) >= m_b^2 < O_8^{\Upsilon(1S)}(^1S_0) >$ and defining the ratio

$$r(p_T) \;=\; \frac{\sum_{J=0}^{2}\frac{d\sigma}{dp_T}[^3P_J^{(8)}]}{\frac{d\sigma}{dp_T}[^1S_0^{(8)}]} \tag{7}$$

it is found $r \simeq 5$ as a mean value over the $[0, 20]$ GeV p_T-range. Actually the above ratio is not steady as a function of the $\Upsilon(1S)$ transverse momentum. Therefore in the generation we splitted the p_T region into two domains: for $p_T \leq 6$ GeV we set $r = 6$ whereas for $p_T > 6$ GeV we set $r = 4$.

In summary, only the $^1S_0^{(8)}$ channel was generated but rescaled by the factor r to incorporate the $^3P_J^{(8)}$ contribution as we did in [4] for charmonium hadroproduction. Consequently, in analogy to [11] we shall derive a numerical estimate for the combination of the colour-octet matrix elements:

$$\frac{< O_8^{\Upsilon(1S)}(^1S_0) >}{5} + \frac{< O_8^{\Upsilon(1S)}(^3P_0) >}{m_b^2}$$

2.2 Altarelli-Parisi evolution

According to the colour-octet model, gluon fragmentation becomes the dominant source of heavy quarkonium direct production at high transverse momentum. On the other hand, Altarelli-Parisi (AP) evolution of the splitting gluon into $(Q\overline{Q})$ produces a depletion of its momentum and has to be properly taken into account. If not so, the resulting long-distance parameter for the ${}^3S_1^{(8)}$ channel would be underestimated from the fit [14].

The key idea is that AP evolution of the fragmenting gluon is performed from the evolution of the *gluonic partner* of quarkonium in the final state of the production channel

$$g \ + \ g \rightarrow g^*(\rightarrow (Q\overline{Q})[{}^3S_1^{(8)}]) \ + \ g \tag{8}$$

Let us remark that, in fact, g^* is not generated in our code [4]. Final hadronization into a $(Q\overline{Q})$ bound state is taken into account by means of the colour-octet matrix elements multiplying the respective short-distance cross sections [11, 4]. Nevertheless, it is reasonable to assume that, on the average, the virtual g^* should evolve at high p_T similarly to the other final-state gluon - which actually is evolved by the PYTHIA machinery. We used this fact to simulate the (expected) evolution of the (ungenerated) g^* whose momentum was assumed to coincide with that of the resonance (neglecting the effect of emission/absorption of soft gluons by the intermediate coloured state bleeding off colour [5]).

Therefore, event by event we get a correcting factor to be applied to the transverse mass of the $(Q\overline{Q})$ state (for the ${}^3S_1^{(8)}$ channel only):

$$x_p \ = \ \frac{\sqrt{P_T^{*2} + m^2_{(Q\overline{Q})}}}{\sqrt{P_T^2 + m^2_{(Q\overline{Q})}}} \tag{9}$$

where P_T (P_T^*) denotes the transverse momentum of the final-state gluon without (with) AP evolution and $m_{(Q\overline{Q})}$ denotes the mass of the resonance. At high p_T,

$$p_T^{AP} \ = \ x_p \times p_T \tag{10}$$

where p_T is the transverse momentum of the resonance as generated by PYTHIA (i.e. without AP evolution), whereas for $p_T \leq m_{(Q\overline{Q})}$ the effect becomes much less significant as it should be. Thus the interpolation between low and high p_T is smooth with the right asymptotic limits at both regimes.

The above way to implement AP evolution may appear somewhat simple but it remains in the spirit of our whole analysis, i.e. using PYTHIA machinery whenever possible. In fact, it provides an energy depletion of the fragmenting gluon in accordance with Cho and Leibovich's work for charmonium hadroproduction [11, 14]. It is worth to note, moreover, that the effect of the AP evolution on the generation over the [0,20] GeV p_T-range, though sizeable, is considerably less pronounced for bottomonium than for charmonium because of the larger mass of the former.

Notice finally that, although we can switch on/off AP evolution and initial-state radiation *at will* in the generation, both next-to-leading order effects have to be incorporated for a realistic description of the hadronic dynamics of the process.

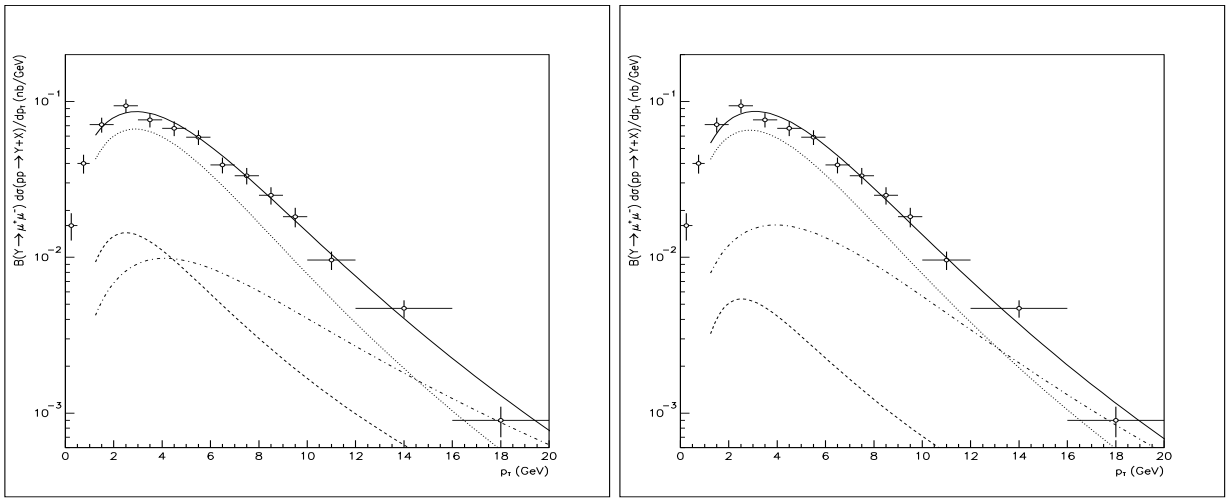

Figure 1: Theoretical curves obtained from a fit using PYTHIA including the colour-octet mechanism for prompt $\Upsilon(1S)$ production against CDF data at the Tevatron *a)* without AP evolution of the fragmenting gluon, *b)* with AP evolution of the fragmenting gluon. The CTEQ2L parton distribution function and $m_b = 4.88$ GeV were employed in the fits; dotted line: CSM, dashed line: ${}^1S_0^{(8)} + {}^3P_J^{(8)}$ contribution, dot-dashed line: ${}^3S_1^{(8)}$ contribution, solid line: all contributions.

3 Fit to Tevatron data

As already mentioned, the theoretical differential cross section on inclusive production of prompt $\Upsilon(1S)$'s stands above Tevatron experimental points for relatively high p_T if the set of long-distance parameters from [11] are blindly employed in the PYTHIA generation with initial-state radiation on. Therefore we performed a new fit to recent CDF data, incorporating both direct and indirect production through the CSM (as a "fixed" contribution) which, in fact, is dominant at low and even moderate p_T.

3.1 Extraction of the colour-octet MEs

In order to assess the effect of AP evolution on the fit parameters we show in table 1 two sets of numerical values for the relevant colour-octet MEs obtained from a best χ^2 fit to Tevatron data [12] using the CTEQ2L PDF: (i) the first row corresponds to a generation *without* AP evolution; (ii) the second set does take it into account. Notice the increase of $< O_8^{\Upsilon(1S)}({}^3S_1) >$ in the latter case w.r.t. AP off (but to a lesser extent than for charmonium [14]) whereas $M_5^{\Upsilon(1S)}$ decreases consequently to keep the fit at low and moderate p_T values.

Let us stress that our MEs numerical estimates have to be viewed with some caution because of the theoretical and "technical" (due to the Monte Carlo assumptions) uncertainties. For example our algorithm for AP evolution should be regarded as a way to reasonably steepening the high-p_T tail of the (leading-order) differential cross section which otherwise would fall off too slowly as a function of p_T.

Table 1: Colour-octet matrix elements (in units of 10^{-3} GeV^3) from the best fit to CDF data at the Tevatron on prompt $\Upsilon(1S)$ production. The CTEQ2L PDF was used with initial-state radiation on, and AP evolution off and on respectively. For comparison we quote the values given in [16, 11]: 480 and 40±60 respectively.

ME:	$< O_8^{\Upsilon(1S)}(^3S_1) >$	$M_5^{\Upsilon(1S)} = 5\times\left(\frac{<O_8^{\Upsilon(1S)}(^3P_0)>}{m_b^2} + \frac{<O_8^{\Upsilon(1S)}(^1S_0)>}{5}\right)$
AP off	93±18	17±20
AP on	139±31	6±18

In figure 1 we show the theoretical curves obtained from our fit to CDF data (independently with AP evolution off and on in the generation) for both colour-singlet and colour-octet contributions. Let us remark that due to the p_T cut-off parameter set in the generation, only those experimental points with $p_T > 1$ GeV were used in the fit. Very good fits, with χ^2/N_{DF} values close to unity, were found.

3.1.1 Separated production sources for $p_T > 8$ GeV

Current statistics does not permit to subtract indirect production sources to obtain the direct $\Upsilon(1S)$ production cross section along the full accessible p_T-range. Nevertheless, feeddown from higher states ($\Upsilon(nS)$, $\chi_{bJ}(nP)$) was experimentally separated out for $p_T >$ 8 GeV [13]. We use this information to check our analysis *a posteriori* (rather than using it as a constraint in the generation) and to draw some important conclusions. To this end the relative fractions of the contributing channels for $p_T > 8$ GeV are reproduced in table 2 from Ref. [13]. On the other hand we show in table 3 the fractions found in this work corresponding to the different generated channels for $p_T > 8$ GeV, following the notation introduced in section 2.1.

Table 2: Relative fractions (in %) of the different contributions to $\Upsilon(1S)$ production from CDF data at $p_T > 8$ GeV [13]. Statistical and systematic errors have been summed quadratically.

contribution	Tevatron results
direct $\Upsilon(1S)$	51.8±11.4
$\Upsilon(2S)$+$\Upsilon(3S)$	10.7±6.4
$\chi_b(1P)$	26.7±8.1
$\chi_b(2P)$	10.8±4.6

By comparison between tables 2 and 3 we can conclude that the $\Upsilon(1S)$ indirect production from χ_{bJ}'s decays is almost completely accounted for by the CSM according to the assumptions and values of the parameters presented in Section 2. Indeed, experimentally 37.5±9.3% of $\Upsilon(1S)$ production is due to $\chi_{bJ}(1P)$ and $\chi_{bJ}(2P)$ decays [13] while from our

Table 3: Relative fractions (in %) of the different contributions to $\Upsilon(1S)$ production at the Tevatron for $p_T > 8$ GeV from our generation. Possible contributions from $\chi_{bJ}(3P)$ states were not generated.

contribution	our generation
$\Upsilon(1S)\vert_{^3S_1^{(8)}}$	42.3
$\Upsilon(1S)\vert_{^1S_0^{(8)}+^3P_J^{(8)}}$	3.7
$\Upsilon(1S)\vert_{CSM}$	14.9
$\Upsilon(2S)+\Upsilon(3S)\vert_{CSM}$	3.0
$\chi_b(1P)\vert_{CSM}$	21.4
$\chi_b(2P)\vert_{CSM}$	14.7

generation we find a close value, namely 36.1%, coming exclusively from colour-singlet production! Moreover, assuming that a 7.7% from the 42.3% fraction corresponding to the colour-octet $^3S_1^{(8)}$ contribution (as expressed in Eq. (6)) can be attributed to the $\Upsilon(2S) + \Upsilon(3S)$ channel in addition to the colour-singlet contribution (3%), we obviously get the fraction 10.7% for the latter, bringing our theoretical result into agreement with the experimental value. Furthermore, this single assignment implies to reproduce very well the experimental fraction ($\approx 52\%$) of direct $\Upsilon(1S)$ production by adding the remaining $^3S_1^{(8)}$ contribution to the $\Upsilon(1S)\vert_{^1S_0^{(8)}+^3P_J^{(8)}}$ and $\Upsilon(1S)_{CSM}$ channels ($\approx 53\%$).

Of course all the above counting was based on mean values from table 2 and subject to uncertainties. Nevertheless, apart from the consistency of our generation w.r.t. experimental results under minimal assumptions, we can conclude, as an important consequence, that there is almost *no need for* $\Upsilon(1S)$ indirect production from feeddown of χ_{bJ} states produced through *the colour-octet mechanism*. In other words, the relative contribution from P-wave states to $< O_8^{\Upsilon(1S)}(^3S_1) > |_{tot}$ in Eq. (6) should be quite smaller than naïvely expected from NRQCD scaling rules compared to the charmonium sector, in agreement with some remarks made in [16]. The underlying reason for this discrepancy w.r.t other analyses [11] can be traced back to the dominant colour-singlet contribution to the cross section at p_T values as much large as 14 GeV (see figure 1) caused by the effective k_T smearing - already applied to charmonium hadroproduction by one of us [4].

On the other hand the corresponding velocity scaling rule in the bottomonium sector is nicely verified. Indeed from the value $< O_1^{\Upsilon(1S)}(^3S_1) > |_{tot} = 11.1$ GeV^3 and the result found for $< O_8^{\Upsilon(1S)}(^3S_1) > |_{tot} = 0.139$ GeV^3 shown in table 1, the ratio

$$\frac{< O_8^{\Upsilon(1S)}(^3S_1) > |_{tot}}{< O_1^{\Upsilon(1S)}(^3S_1) > |_{tot}} \approx 0.012 \tag{11}$$

is in accordance with the expected order of magnitude $\approx v^4$, where v is the relative velocity of the bottom quark inside bottomonium ($v^2 \approx 0.1$).

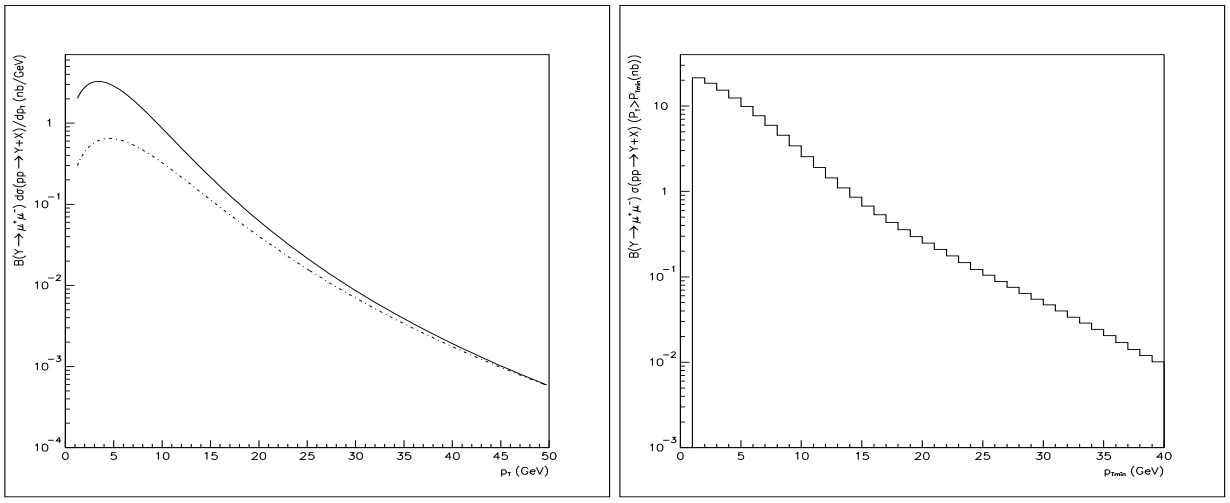

Figure 2: *left :* Predicted prompt $\Upsilon(1S)$ differential cross section at the LHC using the CTEQ2L PDF and AP evolution incorporated in the generation. A rapidity cut $|y| < 2.5$ was required for bottomonium; dot-dashed line: ${}^3S_1^{(8)}$ contribution. Solid line: all contributions. *right :* Integrated cross section.

4 $\Upsilon(1S)$ Production at the LHC

Bottomonium hadroproduction is especially interesting to check the validity of the colour-octet model as often emphasized in the literature [18, 19]. This becomes particularly clear at the LHC since experimental data will spread over a wider p_T-range than at the Tevatron.

Keeping this interest in mind, we generated prompt $\Upsilon(1S)$ resonances in proton-proton collisions at a center-of-mass energy of 14 TeV by means of our code implemented in PYTHIA employing the same colour-octet MEs of table 1 with AP evolution on. We present in figure 2 our theoretical curves for the $\Upsilon(1S)$ differential and integrated cross sections as a function of p_T, including both direct production and feeddown from higher resonance states.

In figure 3 we show our prediction for *direct* $\Upsilon(1S)$ production. This is especially interesting if LHC detectors will be able to discriminate among such different sources of resonance production. To this end we generated $\Upsilon(1S)$ events through both the CSM and COM making use of the following parameters

- $< O_1^{\Upsilon(1S)}({}^3S_1) > |_{direct} = 9.28$ GeV^3 (from [16])
- $< O_8^{\Upsilon(1S)}({}^3S_1) > |_{direct} = 0.114$ GeV^3
- $M_5^{\Upsilon(1S)} = 6.0$ GeV^3

The first value corresponds to the CSM ME for direct production. The $< O_8^{\Upsilon(1S)}({}^3S_1) >$ ME was obtained after removing the $\Upsilon(2S) + \Upsilon(3S)$ contribution according to the discussion made in section 3.1.1, i.e. under the assumption that a fraction 7.7% from the 42.3% in table 3 should be assigned to indirect production. Finally the $M_5^{\Upsilon(1S)}$ value is based on the assumption that this channel mainly contributes to direct production.

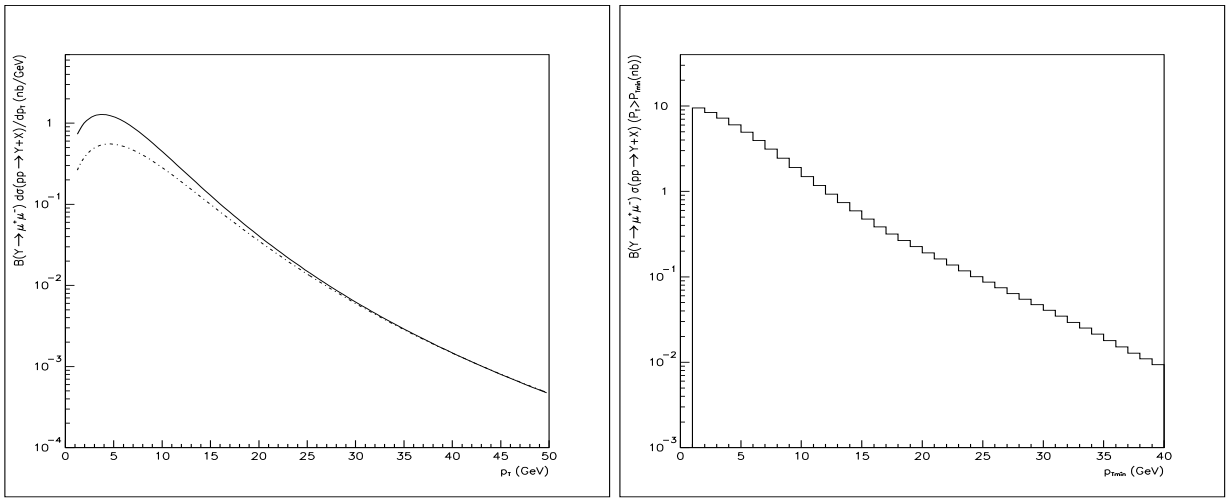

Figure 3: The same as in figure 2 for *direct* $\Upsilon(1S)$ production at the LHC.

5 Summary

In this paper we have analyzed CDF measurements on $\Upsilon(1S)$ production cross sections at the Tevatron in a Monte Carlo framework. Higher-order QCD effects such as initial-state radiation of gluons and AP evolution of splitting gluons into $(b\overline{b})$ states were taken into account. On the other hand, since different sources of $\Upsilon(1S)$ production were not experimentally separated along the full accessible p_T-range we have included all of them in the generation and later fit. Only for $p_T > 8$ GeV feeddown from χ_{bJ} states was experimentally separated out from direct production. We used such results as a consistency check of our analysis and to draw some conclusions summarized below.

The numerical value of the $< O_8^{\Upsilon(1S)}(^3S_1) > |_{tot}$ matrix element should be ascribed almost totally to $\Upsilon(nS)$ states. This finding may be surprising when confronted with other results obtained from previous analyses [11, 16], where the contribution to the $\Upsilon(1S)$ yield through the colour-octet χ_{bJ} channels was thought as dominant [16, 20, 19]. On the contrary, we concluded from tables 2 and 3 that the *colour-singlet production* by itself can account for the feeddown of $\Upsilon(1S)$ from χ_{bJ} states. (Notice however that experimental uncertainties still leave some room for a possible COM contribution but to a much lesser extent than previously foreseen [11, 16].) On the other hand the different production channels are consistent (or can be made consistent) with the experimental relative fractions shown in table 2, after some reasonable assumptions.

We have extended our study to LHC collider experiments ($\sqrt{s} = 14$ TeV center-of-mass energy). In figure 2 we present our predictions for prompt production rates (i.e. including direct and indirect production) while in figure 3 we show our prediction for direct production alone.

Lastly we conclude that the foreseen yield of $\Upsilon(1S)$'s at LHC energy will be large enough even at high-p_T to perform a detailed analysis of the colour-octet production mechanism and should be included in the B-physics programme of the LHC experiments, probably deserving (together with charmonia) a dedicated data-taking trigger.

Acknowledgments

We acknowledge the working subgroup on b-production of the Workshop on the Standard Model (and more) at the LHC, especially M. Kraemer and M. Mangano, for comments and valuable discussions. We also thank R. Cropp and G. Feild for their assistance on some experimental issues concerning bottomonia production at the Tevatron.

References

[1] ATLAS detector and physics performance Technical Design Report, CERN/LHCC/99-15.

[2] M.A. Sanchis-Lozano and B. Cano, Nucl. Phys. B (Proc. Suppl.) 55A (1997) 277.

[3] B. Cano-Coloma and M.A. Sanchis-Lozano, Phys. Lett. **B406** (1997) 232.

[4] B. Cano-Coloma and M.A. Sanchis-Lozano, Nucl. Phys. **B508** (1997) 753.

[5] M.A. Sanchis-Lozano, Nucl. Phys. B (Proc. Suppl.) 75B (1999) 191.

[6] T. Sjöstrand, Comp. Phys. Comm. **82** (1994) 74.

[7] E. Braaten and S. Fleming, Phys. Rev. Lett. **74** (1995) 3327.

[8] G.T. Bodwin, E. Braaten, G.P. Lepage, Phys. Rev. **D51** (1995) 1125.

[9] G. Schüler, CERN-TH -7170-94, hep-ph/9403387.

[10] CDF Collaboration, Phys. Rev. Lett. **69** (1992) 3704.

[11] P. Cho and A.K. Leibovich, Phys. Rev. **D53** (1996) 6203.

[12] G. Feild *et al.*, CDF note 5027.

[13] CDF Collaboration, CDF note 4392.

[14] M.A. Sanchis-Lozano, Montpellier QCD Conference, hep-ph/9907497.

[15] C. Caso *et al.*, Particle Data Group, EPJ **C3** (1998) 1.

[16] G. Schüler, Int. J. Mod. Phys. **A12** (1997) 3951.

[17] E.J. Eichten and C. Quigg, Phys. Rev. **D52** (1995) 1726.

[18] M. Beneke and M. Krämer, Phys. Rev. **D55** (1997) 5269.

[19] A. Tkabladze, DESY preprint 99-082, hep-ph/9907210.

[20] M. Beneke, CERN-TH/97-55, hep-ph/9703429.